JTTEE5 9:114-120
© ASM International

Peer Reviewed

Design of a New Nozzle for Direct Current Plasma Guns with Improved Spraying Parameters

M. Jankovic, J. Mostaghimi, and V. Pershin

(Submitted 15 October 1998; in revised form 22 May 1999)

A new design is proposed for direct current plasma spray gas-shroud attachments. It has curvilinearly shaped internal walls aimed toward elimination of the cold air entrainment, recorded for commercially available conical designs of the shrouded nozzle. The curvilinear nozzle design was tested; it proved to be capable of withstanding high plasma temperatures and enabled satisfactory particle injection. Parallel measurements with an enthalpy probe were performed on the jet emerging from two different nozzles. Also, corresponding calculations were made to predict the plasma flow parameters and the particle parameters. Adequate spray tests were performed by spraying iron-aluminum and MCrAlY coatings onto stainless steel substrates. Coating analyses were performed, and coating qualities, such as microstructure, open porosity, and adhesion strength, were determined. The results indicate that the coatings sprayed with a curvilinear nozzle exhibited lower porosity, higher adhesion strength, and an enhanced microstructure.

Keywords argon plasma jets, thermal spraying, shrouded nozzle

1. Introduction

Gas-shrouded nozzles are used as attachments for conventional spray guns with a twofold purpose: (a) to inject secondary (shrouding) gas to reduce the mixing of the plasma with the surrounding atmosphere and (b) to extend the hot core of the jet by rearranging the gas flow to increase the dwell time of particles in the plasma. To fulfill the latter, gas-shrouded nozzles are usually built in the shape of a divergent conical diffuser. This type of nozzle design is believed to provide plasma flow parameters, resulting in a prolonged dwell time of the particles, and helps to avoid the clogging problem characteristic of internal particle injection. However, conical gas-shrouded nozzles suffer from the entrainment problem. Surrounding air is pumped along the walls of the nozzle, spoiling the plasma parameters to a certain extent. In parametric studies performed on gas-shrouded nozzles,[1] it was found that the amount of entrained air depends on the cone angle and the flow rate of plasma. Similar results were published by Betoule *et al.*[2] They reported entrainment problems for conical nozzles with angles of 6° and greater.

Based on a parametric study,[1] a new curvilinear nozzle design was suggested. The aim is to eliminate cold air entrainment, while maintaining some advantages of the conical nozzles such as plasma deceleration and an increased dwell time of the particles.

The schematic of the spraying gun, with a conical shrouded nozzle attachment, is given in Figure 1(a), where the angle of the commercial nozzle was $\alpha = 10.7°$. The curvilinear nozzle design was based on the analysis of streamlines inside the conical nozzle. The concept was to shape the nozzle in such a way that its wall profile coincided with the particular flow streamline, which represented the total argon flow. The angle of the conical section ($\alpha = 10.7°$) and the length of the nozzle remained constant (Figure 1b).

M. Jankovic, J. Mostaghimi, and **V. Pershin,** Department of Mechanical and Industrial Engineering, University of Toronto, Toronto, ON, Canada M5S 1A4. Contact e-mail: mostag@mie.utoronto.ca.

The new curvilinear nozzle was manufactured and proved to be a compact, well-cooled unit, capable of withstanding the most rigorous spraying tests. No signs of erosion or any other damage were found after several hours of operation. The internal nozzle surface maintained its original copper color after hours of testing, whereas the conical design developed a layer of oxides with a characteristic green color. This indicates that the curvilinear nozzle was free from air entrainment, which is in agreement with the streamline analysis performed.[1]

A series of spray tests was carried out on both nozzles, the conical and the curvilinear, and the coatings obtained were analyzed. In addition, a detailed analysis of the particle behavior was performed for both nozzles. Particle trajectories, velocities, and temperature histories were calculated to correlate these parameters to the quality of the coatings obtained. Particle velocity measurements were performed using particle image velocimetry, with an external illumination by pulsed lasers. The images were recorded using a CCD digital camera (COHU 4910, COHU Inc., San Diego, CA), and the spray was illuminated by two laser pulses. A thin sheet of laser light was produced by passing the light of the nitrogen lasers ($\lambda = 337$ nm) through a cylindrical lens. The camera was both filtered and intensified to reduce the background radiation emanating from the plasma. A double image of each particle was captured in a single frame, and from the distance between images, a particle velocity was calculated.

Temperature measurements were performed with a ratio pyrometer by reading the ratio of radiation emitted by the particles at two different wavelengths. The radiation was split by a bifurcated optic cable and delivered to two photomultipliers (Hamamatsu HC120, Hamatsu Corp., Bridgewater, NJ) through filters at wavelengths of 681 and 850 nm. The apparatus was built at the University of Toronto and is described elsewhere.[3,4] The results are summarized in the following sections.

2. Plasma Jet Parameters

Spraying tests were performed using the plasma gun SG-100 (Miller Thermal Inc., Appleton, WI), operating at $P_{el} = 19.6$ kW

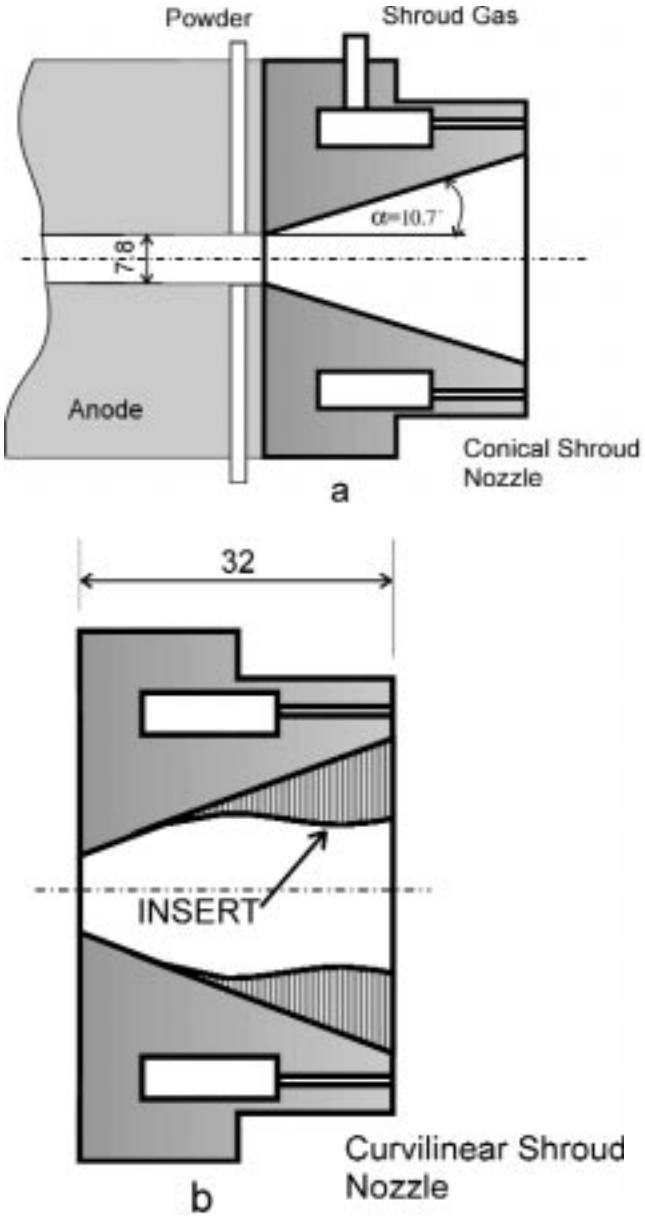

Fig. 1 Schematics of the (**a**) conical and (**b**) curvilinear nozzles.

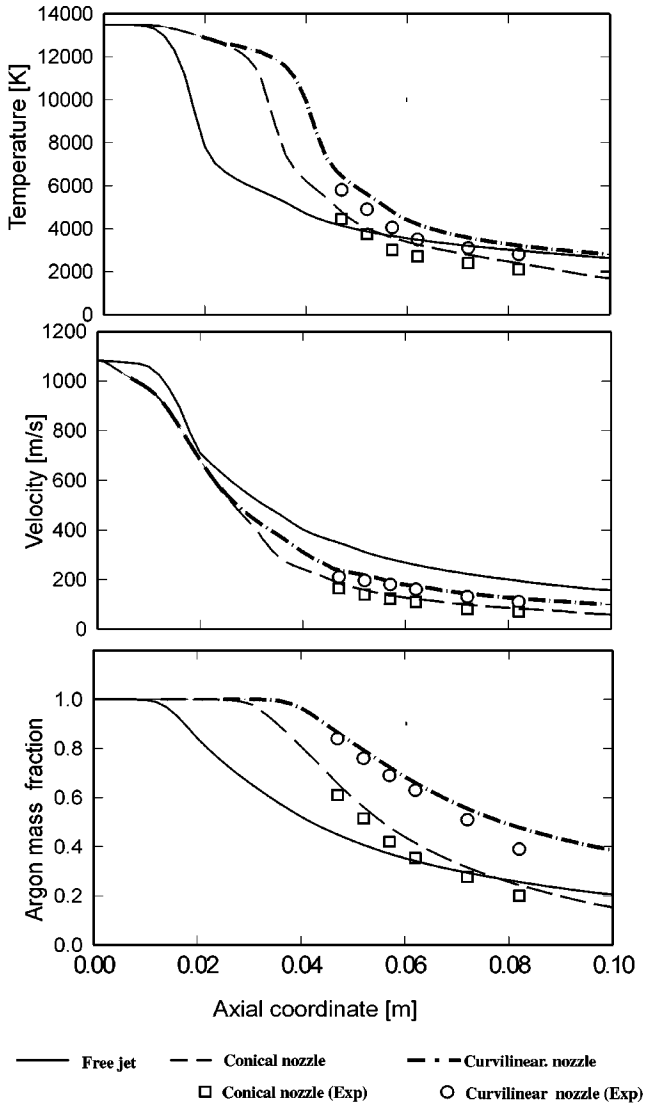

Fig. 2 Axial distribution temperature, velocity, and argon concentration in plasma. Calculations and measurements.

($U = 28$ V, $I = 700$ A), with an argon flow rate of $\dot{m} = 1$ g/s. The torch was equipped with anode, 2083-175; cathode, 1083A-129; and gas injection, 2083-130. The velocity and temperature distributions of the resulting plasma flow presented the driving force for particle heating and acceleration toward the substrate. For this reason, the major parameters of the plasma flow, such as velocity, temperature, and argon concentration, were determined experimentally and numerically.

Experimental results were obtained using the enthalpy probe method [5,6,7] at discrete locations throughout the jet. Numerical results were obtained by solving equations governing the conservation of mass, momentum, and energy. The standard k-ε model of turbulence was used, which allows completion of the system of conservation equations by including kinetic energy of turbulence, k, and its dissipation ε, and adjusted for this specific flow geometry.[1,7] Figure 2 presents these results in terms of axial distribution of velocity, temperature, and argon mass fraction for three different cases: free jet (without shrouded nozzle), curvilinear, and conical nozzles. Also, experimental results obtained by the enthalpy probe are given for the curvilinear and conical nozzles.

The agreement between calculated parameters and experimental measurements is relatively good. The curvilinear nozzle yields much higher temperatures for most of the flow domain. It was found that the jet emerging from the curvilinear nozzle is brighter and longer, possibly signifying higher plasma temperatures. The particle temperatures are also higher because the vaporization from the surface of some particles was observed at a distance of 12 to 20 mm from the nozzle exit (Figure 3). In the case of the conical nozzle, there is no surface vaporization, so the particles must have had lower temperatures. Also, the argon fraction remains higher throughout the region (Figure 2), which is an important consideration for metallic powders that may otherwise oxidize.

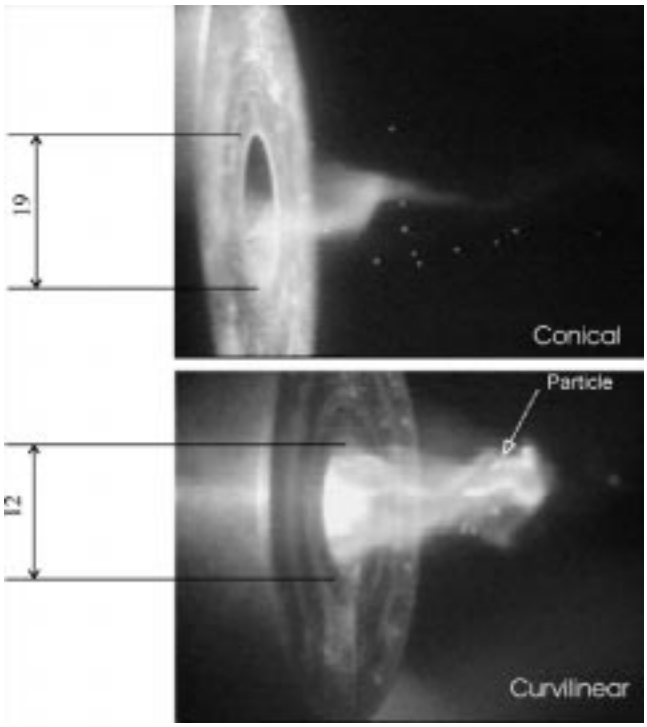

Fig. 3 Images of particles at the exit of the two nozzles (dimensions in millimeters).

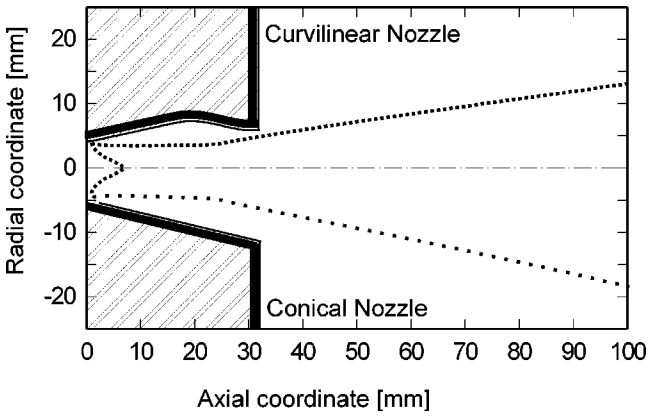

Fig. 4 Envelopes of particle trajectories for both nozzles.

The difference in gas velocity for two nozzles is not very significant, but it is evident that both nozzles provide plasma gas deceleration to a certain extent. Both nozzles improve the plasma parameters compared to the free jet, because mixing with the surrounding air is fully eliminated in the case of the curvilinear nozzle and restricted in the case of the conical nozzle.

3. Particle Behavior

Injection of the particles is an important part of the spray process. The location and number of injection ports, the flow rate of the carrier gas, and the particle feed rate need to be carefully chosen to ensure proper particle trajectory. Generally, there are two types of injection, internal and external. With external injection, the plasma carries the particles away from the gun and there is no chance of melted particles striking the cold nozzle walls. Conversely, they have a relatively short residence time in the plume for melting and acceleration. When spraying with gas-shrouded nozzles, the internal injection mode is generally used, with the particle injection point located inside the nozzle. Thus, the particles have a longer time available to heat up and accelerate toward the substrate. The major problem with internal injection is adjusting the particle trajectories and their accumulation on the nozzle walls. The injection velocity should be high enough to ensure sufficient penetration of the particle into the hottest zone of plasma, but not excessive, or this will result in particles traveling across the channel and hitting the opposite wall.

The trajectories of the injected particles can be calculated by establishing the balance of forces that the thermal plasma flow exerts on the individual particle. Many forces act upon a single particle traveling into the fluid flow,[8,9] such as viscous drag force, gravity force, thermophoresis, the Basset history term, electromagnetic force, and so on. Their relative importance depends on the particle size distribution and also on the main flow parameters. In their analysis of thermal plasma reactors, Lee and Pfender[10] provided detailed analysis on particle dynamics and suggested an algorithm for calculating the trajectory of an individual particle, which is used in this work. The nature of turbulent flows is stochastic, and in practice, particles of the same size and injection parameters will not follow the same path. Therefore, a stochastic approach is needed to account for the dispersion of particle trajectories due to turbulence. However, the results of our calculations showed that for the size distribution characteristic for plasma spraying (40 to 80 μm), the influence of plasma turbulence on particle trajectories is not strong.

Spray tests were performed with FeAl (Amtech, Amorphous Metal Technologies, Inc., Irvine, CA) and MCrAlY (Amdry 9954, Sultzer-Metco Inc., Westbury, NH) powders, with spherical particle shape and a size distribution of 37 to 75 μm. The particle injection velocity (7.2 m/s) was based on the optimum carrier gas flow rate necessary for transport from the powder feeder to the injection port, and the feed rate was 20 g/min. The spray gun parameters were identical to those in enthalpy probe measurements in "Plasma Jet Parameters," and the spray distance was $x = 100$ mm.

Envelopes of the trajectories were obtained by using the average trajectories for the particles from the upper and lower limits of the size distribution. They are presented in Figure 4 for the curvilinear and conical nozzles. The envelope was 20% narrower for the curvilinear nozzle. This was also confirmed by the particle flow visualization during the spray tests. The results show that for both nozzles, for a given injection velocity, the envelopes of the trajectories do not intersect the wall. In the case of the curvilinear nozzle, the edge of the envelope is much closer to the nozzle wall at the exit, making it more sensitive to the changes in injection parameters.

The results of particle velocity measurements are presented in Figure 5 in terms of particle velocity distribution on the centerline for the two nozzles. Analysis showed particle velocities were of the same order of magnitude for both nozzles, but the velocity distribution of particles from the curvilinear nozzle is slightly shifted toward the higher velocity region.

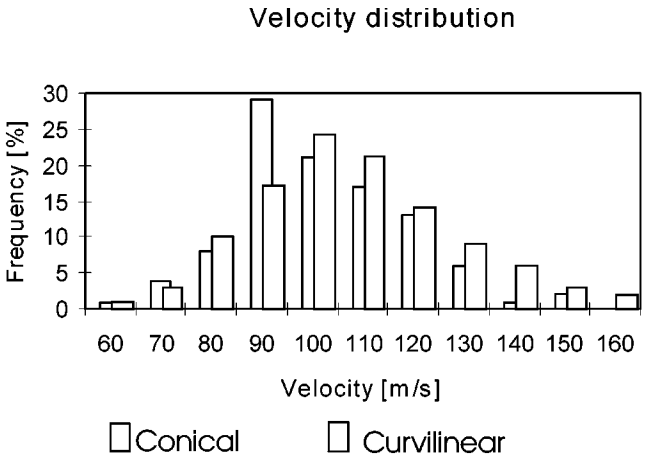

Fig. 5 Particle velocity distribution at spraying distance of 100 mm for the two nozzles.

4. Particle Temperature

Upon injection, a particle is subjected to intense heating from the plasma. As the temperature of the particle increases, the heat loss by radiation from the particle becomes more important, and the net heat transfer from plasma to the particles is the balance between these two processes. Calculating the temperature field of the particles becomes a complex task, considering the different shapes of the individual particles, with the resulting irregular temperature distributions inside the particles as well as the time dependence of the overall process. Some simplifications and assumptions are needed to form a closed set of differential equations that represent the heat and mass transfer of a single particle. Calculations were based on the Lee and Pfender[10] algorithm for particle temperature evaluations.

Coating quality depends on a combination of injection and plasma parameters that govern the particle melting prior to impact. This is a complex phenomenon because the various size particles behave differently upon injection. The heating of a single particle strongly depends on the drag force, because it defines the particle trajectory and its residence time in the plasma. Equally important are the particle size and its physical properties, for example, heat and temperature of melting. The following assumptions were made to simplify the problem:[10] (a) solid and molten particles were spherical in shape; (b) internal conduction of the particle was negligible; and (c) vaporization from the free surface of the molten particle, charging, noncontinuum effects, and the effect of strongly varying plasma properties were neglected.

Temperature histories for three different particle sizes were calculated and are presented in Figure 6 for curvilinear and conical nozzles. Additionally, results of temperature measurements for the particle size range +37 to 67 μm are shown. Calculations show that upon injection, the particles heat up rapidly until they reach the melting point. Corresponding particles sprayed by the curvilinear nozzle melt faster and have higher temperatures upon reaching the substrate (x = 100 mm), compared to the conical nozzle situation. Moreover, the particles with diameter $d = 75$ μm are not completely melted with the conical nozzle. The previously given results suggest significant improvement in particle heating and

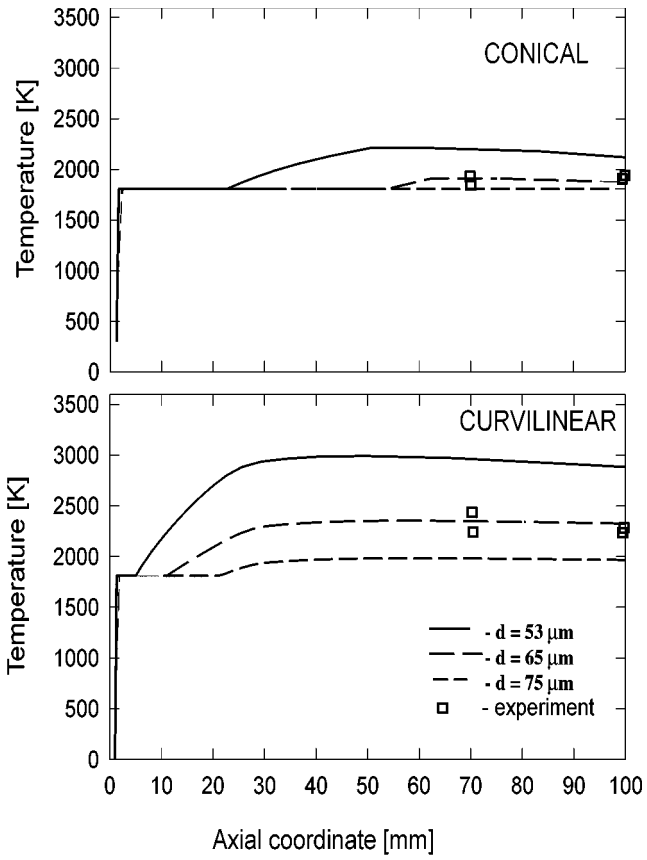

Fig. 6 Temperature histories of the particles.

melting when spraying with the curvilinear nozzle. This is due to the significantly higher plasma temperatures yielded by the curvilinear nozzle. It is also important to notice that none of the particles from this size range have reached the boiling point.

In order to examine the behavior of a large number of the particles, a full stochastic model was used. Results are given in Table 1, as the percentage of completely melted particles for different nozzle configurations. The thermal properties of iron-aluminum powder (90% iron and 10% aluminum) were calculated by applying the mixing rule.

Few particles, less than 2%, remain unmelted with the curvilinear nozzle. When spraying with the conical nozzle, or without a nozzle, a fairly large percentage of the particles remain unmelted, 11.3 and 21.7%, respectively. This can significantly decrease the quality of the coatings, resulting in higher porosity, and lower adhesion and cohesion strengths.

5. Coating Evaluation

Analysis of the coating microstructures was carried out by scanning electron microscopy (SEM), and image analysis was employed for porosity and evaluation of structural features.

To avoid additional defects during specimen preparation, such as grain pull off, the specimens were impregnated with epoxy resin. The choice of SEM over optical microscopy, and the selected magnification (500 to 700×), lowered the error introduced by the threshold level selection for porosity measurement.[11]

Table 1 Percentage of completely melted iron-aluminum particles

Torch configuration	Melted iron-aluminum powder, %
Curvilinear nozzle	98.3
Conical nozzle	88.7
No nozzle	78.3

Figure 7 presents cross sections of the MCrAlY coatings sprayed by the curvilinear and conical nozzles. Clearly, the curvilinear nozzle produced a more uniform microstructure, lamellae of regular shape, which were thin and elongated. The coating sprayed with the conical nozzle has more irregularities, pores, and unmelted spherical particles, the result of insufficient heating.

The shape factor for lamella evaluation was the circularity of its cross section:[12]

$$Circularity = (Perimeter)^2/Area$$

Circularity for a lamella that has a perfectly circular cross section has a minimum value of 4π. Circularity is higher for more elongated cross sections and could reach a value of about 50 for lamella with a 10 to 1 diameter-to-height ratio. Cross sections of iron-aluminum coatings were analyzed with the OPTIMAS 6 image analysis package (Optimas Corp., Bothell, WA).[12] Four lamellae categories were established, with the range of circularity 16 to 20, 20 to 30, 30 to 40, and 40 to 50. Several fields of view were considered to acquire the data: interface, middle, and upper areas of the coatings. Data collected from image analysis represent typically 30 to 35 lamellae per field of view. Results show that the coating sprayed with the curvilinear nozzle has thinner, elongated lamellae with higher values of circularity, which is a result of more favorable spraying conditions, compared to conical (Figure 8).

Porosity tests were performed by the standard Archimedes weighing method[13] and image analysis for the coatings separated from the substrate. The coating samples were applied by the conical and curvilinear nozzles and without the nozzle. Each sample was weighted three times dry and in water, and average porosity values were calculated with an error of 0.1%. The FeAl coating obtained by the curvilinear nozzle exhibited the lowest porosity of 7.8%, whereas the coating formed by the conical nozzle exhibited a porosity of 12.4%. As was expected, the sample sprayed without a nozzle has the highest porosity of 15.3%. These results are consistent with the image analysis results, where the same tendency was found for MCrAlY coating presented on Fig. 6.

The coating adhesion tests were performed according to the ASTM C 633 standard[14] for NiCrAlY coatings. Results demonstrate that better performance coatings were applied by the curvilinear nozzle versus the conical, with average (for four tests) adhesion strengths of 42.0 and 27.2 MPa, respectively. Observation of the fractured specimens showed that separation occurred within the coatings, that is, it was cohesive in nature.

The results of the adhesion strength and porosity tests are in good agreement with the metallographic observation. Insufficient melting when spraying with the conical nozzle resulted in microstructural irregularities, cavities, and embedded spherical particles. Further on, this resulted in higher porosity and lower bonding strength of the coating.

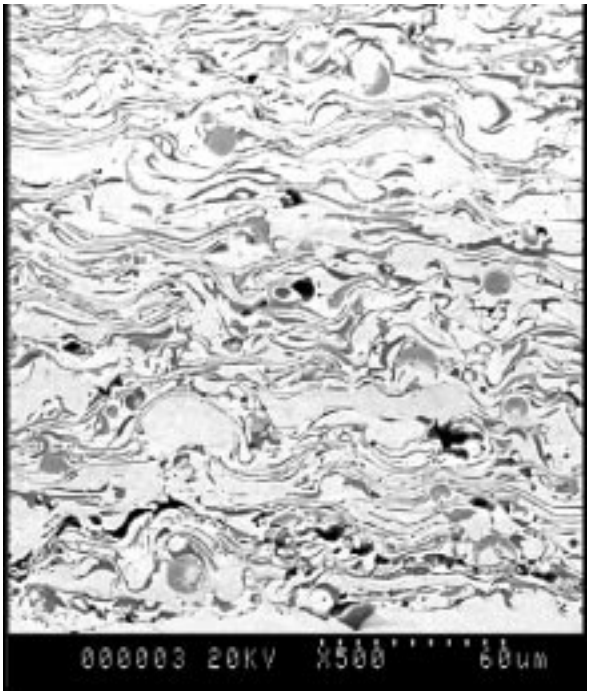

(**a**)

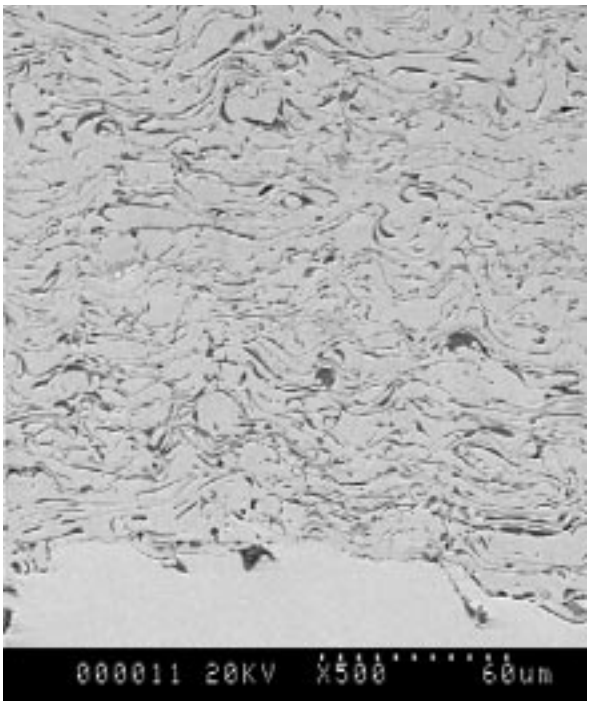

(**b**)

Fig. 7 Cross sections of MCrAlY coatings: (a) conical nozzle, porosity 7 to 7.2%; and (b) curvilinear nozzle, porosity 4.5 to 5.1%.

To characterize the melting behavior of the powder particles during spraying, wipe or single splat tests were performed.[15] The wipe test deposits were laid down in a single horizontal pass of the coupon across the plume. The individual particles were collected

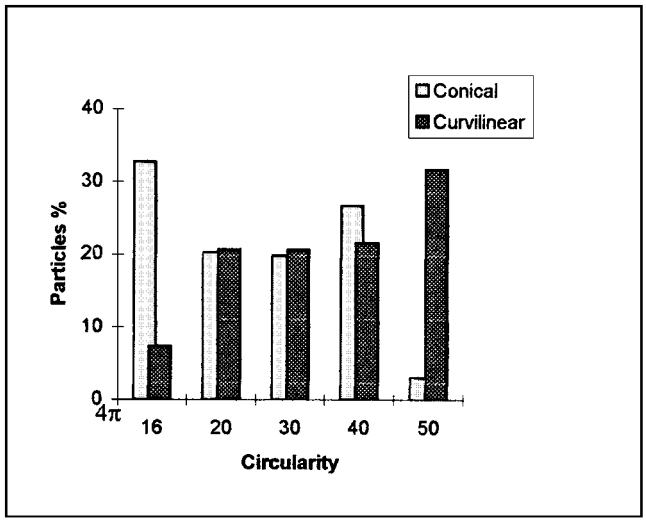

Fig. 8 Circularity of the lamellae within iron-aluminum coating sprayed by two nozzles.

at 100 mm distance and examined by SEM. Figure 9(b) and (c) are typical examples of splats collected at a distance of 100 mm. The splats were sprayed by a conical nozzle with a significant number of unmelted or partially melted particles, some of which have the same surface morphology as the initial powder (Figure 9a), an indication of ineffective heating. The splats sprayed by a curvilinear nozzle show that the particles have almost all fully melted at impact, allowing for better spreading of the splats.

6. Conclusions

A new design of the gas-shrouded nozzle for direct current plasma spraying is presented in this article. It is based on numerical analysis of the streamlines in the standard conical shrouded nozzle. A new shrouded nozzle was built with curvilinear internal walls to eliminate the air entrainment recorded for the conical nozzle. Performance of the gas-shrouded nozzles has been examined by both experimental and numerical analyses. The results show that the curvilinear nozzle gives preferable temperature and argon fraction profiles. This is due to a lack of air entrainment within the nozzle, which could not be avoided by the conical nozzle.

Spraying tests were performed with two different nozzle designs. Coating quality was characterized by measuring the porosity, adhesion, and metallography and single splat tests. The results were used to correlate the quality of the coating to the plasma parameters yielded by the gas-shrouded nozzles. The spray tests indicated improvements in the quality of sprayed coatings. It was found that the coatings sprayed with curvilinear nozzle have lower porosity, better bonding strength, and better microstructure. These differences could be attributed to better plasma flow parameters, significantly higher temperature and argon fraction, and slightly higher velocity. Similar velocities in the free jet region indicate that the dwell time of the particles is approximately the same for the two nozzles. At the same time, in the case of the curvilinear nozzle, a much higher temperature and argon concentration resulted in better particle heating conditions.

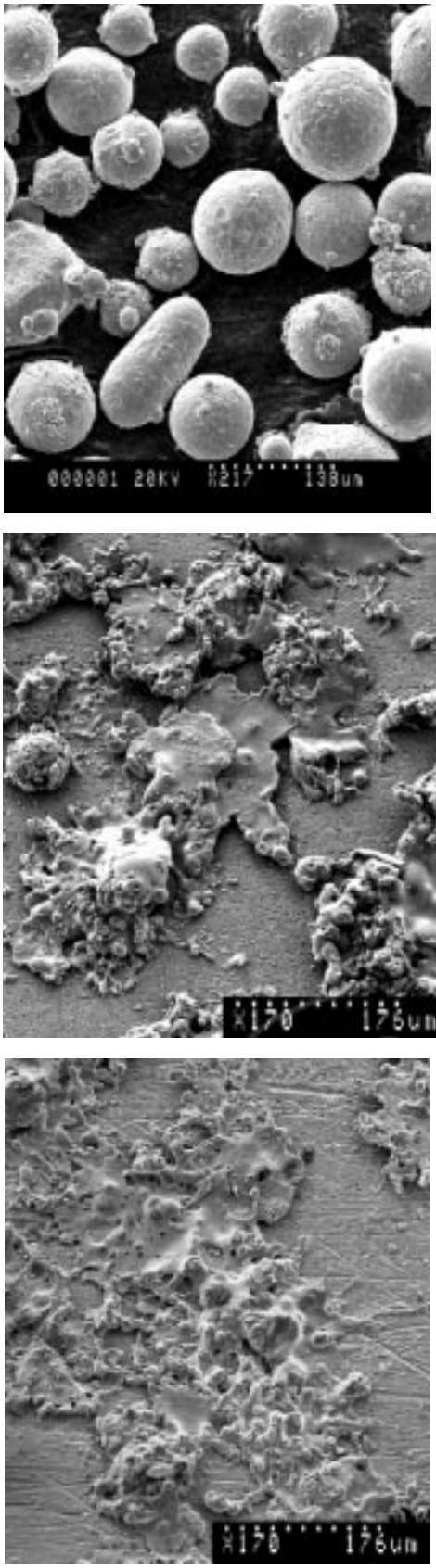

Fig. 9 Micrographs of the **(a)** initial iron-aluminum powder and splats from the **(b)** conical and **(c)** curvilinear nozzle.

Acknowledgments

The financial support of the Ontario Hydro Technology and Ontario Ministry Education and the Training University Research Incentive Fund (URIF) is gratefully acknowledged.

References

1. M. Jankovic and J. Mostaghimi: *Plasma Chem. Plasma Processing*, 1995, vol. 15 (4), pp. 607-28.
2. O. Betoule, A. Denoirjean, J. Coudert, M. Vardelle, and P. Fauchais: in *Thermal Spray Science & Technology*, C.C. Berndt and S. Sampath, eds., ASM International, Materials Park, OH, 1995, pp. 15-19.
3. M. Masri: Master's Thesis, University of Toronto, Toronto, 1996.
4. V. Pershin, J. Mostaghimi, S. Chandra, and T. Coyle: in *Thermal Spray: Meeting the Challenges of the 21st Century*, C. Coddet, ed., ASM International, 1998, pp. 1305-08.
5. J. Grey, P. Jacobs, and M. Sherman: *Rev. Sci. Instrum.*, 1962, vol. 33 (7), pp. 738-41.
6. J. Mostaghimi and E. Pfender: *Proc. ISPC-11, IUPAC*, J. Harry, ed., 1993, vol. 1, pp. 321-26.
7. M. Jankovic: Ph.D. Thesis, University of Toronto, Toronto, 1996.
8. R. Clift, J. Grace, and M. Weber: *Bubbles, Drops and Particles*, Academic Press, New York, NY, 1973.
9. C. Crowe: in *Pulverized Coal Combustion and Gasification*, L. Smoot and D. Pratt, eds., Plenum Press, New York, NY, 1979.
10. Y. Lee, and E. Pfender: *Plasma Chem. Plasma Processing*, 1987, vol. 7 (1), pp. 1.
11. K. Mailhot, F. Gitzohoffer, and M. Boulos: *Thermal Spray: Meeting the Challenges of the 21st Century*, C. Coddet, ed., ASM International, Materials Park, OH, pp. 917-22.
12. *OPTIMAS User Guide*, Version 6, Optimas Co., Bothell, WA, 1996.
13. "Standard Test Method for Density of Glass by Buoyancy," ASTM Designation C 693, ASTM, Philadelphia, PA, 1993, vol. 15.02, pp. 212-14.
14. "Standard Test Method for Adhesion or Cohesive Strength of Flame Sprayed Coatings" ASTM Designation C 633, *19th Annual Book of ASTM Standards*, ASTM, Philadelphia, PA, 1969, part 17, pp. 636-42.
15. W. Smith, T. Jewett, S. Sampath, C.C. Berndt, H. Herman, J. Fincke, and W. Wright: in *Thermal Spray: Practical Solutions for Engineering Problems*, C.C. Berndt, ed., ASM International, Materials Park, OH, 1996, pp. 317-24.